Plumbing the depths of magma crystallization using 176Lu/177Hf in zircon as a pressure proxy

Hugo Moreira, Anda Buzenchi, Chris J Hawkesworth, Bruno Dhuime

GEOLOGY | THE GEOLOGICAL SOCIETY OF AMERICA®

https://doi.org/10.1130/G50659.1

Manuscript received 11 August 2022
Revised manuscript received 24 October 2022
Manuscript accepted 24 October 2022

Published online 3 January 2023

Plumbing the depths of magma crystallization using $^{176}Lu/^{177}Hf$ in zircon as a pressure proxy

Hugo Moreira[1], Anda Buzenchi[1], Chris J. Hawkesworth[2] and Bruno Dhuime[1]
[1]Géosciences Montpellier, Université de Montpellier, CNRS, 34095 Montpellier, France
[2]School of Earth Sciences, University of Bristol, Bristol BS8 1RJ, UK

ABSTRACT

Extensional tectonics are marked by shallow magma crystallization depths, whereas compressional tectonics are associated with deeper crystallization depths. This implies that variations in crystallization depths can be used to track changes in Earth's dominant tectonic regimes through time. We therefore developed a new "pressure of crystallization" proxy based on the variation of the $^{176}Lu/^{177}Hf$ ratio in zircon. This ratio is controlled by zircon fractionation and residual garnet, and it can be used to monitor the evolution of a crystallizing magma ascending within the crust. The secular evolution of the $^{176}Lu/^{177}Hf$ ratio in zircon is characterized by cyclical oscillations that are broadly in tune with the $\delta^{18}O$ record in zircon and with periods of continental collision and supercontinent amalgamation. The apparent mean depth of crystallization of zircon-bearing igneous rocks has decreased with time over the last ~3.0 b.y. This can be linked to shallowing of the primary crystallization depths and/or to the effect of time-integrated erosion in the geologic record. Prior to ca. 3.0 Ga, crystallization depth maxima and oscillations in apparent depth are less clear, perhaps suggesting that the nature of tectonic interactions was different in the Mesoarchean and earlier.

INTRODUCTION

Magmas rise within the continental crust until they stall and solidify (Brown, 1994; Petford et al., 2000; Annen et al., 2006). Their crystallization tends to be shallower in extensional settings than in compressional settings due to contrasting normal stress gradients and conditions of magma propagation (Hogan and Gilbert, 1995; Vigneresse et al., 1999; Loucks, 2021). In geologically young terrains, the crystallization depth of magmas can be measured through geophysical approaches (e.g., Thybo and Nielsen, 2009). However, as a result of erosion and reworking of the crust through time, much of the ancient geologic record has been destroyed. As a consequence, there is little information with which to constrain the depths of crystallization and the periods of crustal extension and compression in the deep geologic past.

Zircon ($ZrSiO_4$) crystallizes from a range of SiO_2-rich magmas, and it is resistant to weathering and erosion processes, such that it is widely preserved in continental sediments across geologic time (Belousova et al., 2010; Voice et al., 2011). Many studies have explored the zircon archive to draw insights into Earth's geodynamic regimes over time (e.g., Belousova et al., 2010; Voice et al., 2011; Dhuime et al., 2012; McKenzie et al., 2018; Balica et al., 2020). These include the use of U-Pb ages to infer the relative volume of magmatism (e.g., Schoene et al., 2012), Hf isotopes as a measure of mantle input and crustal reworking/recycling (e.g., Gardiner et al., 2016), trace-element ratios to infer mean crustal thickness (e.g., Tang et al., 2021), and oxygen isotopes as a proxy for crustal reworking (e.g., Dhuime et al., 2012; Spencer et al., 2014).

Variations in zircon $^{176}Lu/^{177}Hf$ have been documented to describe changes in magma conditions and metamorphic reactions at local scales (e.g., O'Brien and Miller, 2014; Rubatto, 2017), but global data sets of $^{176}Lu/^{177}Hf$ in zircon remain unexplored. Considering that variations in zircon composition may reflect the minerals crystallizing from the host magmas and residues during partial melting, we evaluated the relationship between zircon $^{176}Lu/^{177}Hf$ and pressure. We show that the $^{176}Lu/^{177}Hf$ ratio can be used to ascertain the depth of crystallization of zircon-bearing magmas, and we explore the implications for large-scale tectonic variations through time.

SECULAR EVOLUTION OF $^{176}Lu/^{177}Hf$ IN ZIRCON

Figure 1 shows the variation of the geometric mean of $^{176}Lu/^{177}Hf$ in zircons from a worldwide data set of >120,000 analyses, subdivided into 0.1 b.y. time slices (Data Set S1 in the Supplemental Material[1]). The variation of the zircon $^{18}O/^{16}O$ ratios (expressed as $\delta^{18}O$ relative to Vienna standard mean ocean water [VSMOW]) from an independent global database (Spencer et al., 2014) is plotted for comparison. It is striking that major troughs in $^{176}Lu/^{177}Hf$ correlate with peaks in $\delta^{18}O$, and these in turn broadly coincide with periods of supercontinent assembly. This observation was confirmed by the calculated anomaly in the running means of 0.1 b.y. intervals (inset Fig. 1), with a 0.5–0.6 b.y. cyclicity in $\delta^{18}O$ peaks and $^{176}Lu/^{177}Hf$ troughs at 2.75–2.45 Ga, 2.1–1.9 Ga, 1.3–1.05 Ga, and 0.75–0.55 Ga (as indicated by coherent statistical variations between the two data sets; Tables S1–S5).

Higher values of $\delta^{18}O$ in zircon can be linked to increased assimilation/reworking of supracrustal components and crustal thickening at times of major continental collisions (Spencer et al., 2014). The concomitant lower mean values of $^{176}Lu/^{177}Hf$ during periods of higher $\delta^{18}O$ may similarly reflect crustal thickening and collisional tectonics.

Horizontal compression inhibits the ascent of magmas within the crust (Loucks, 2021), and crustal thickening expands the garnet stability field (e.g., Taylor et al., 2016; Rubatto, 2017). Given that Lu partitions preferentially into garnet, crustal thickening and an expanded garnet

[1]Supplemental Material. Supplemental information, Figures S1–S5, Tables S1–S9, and Data Sets S1–S4. Please visit https://doi.org/10.1130/GEOL.S.21669482 to access the supplemental material and contact editing@geosociety.org with any questions.

CITATION: Moreira, H., et al., 2023, Plumbing the depths of magma crystallization using $^{176}Lu/^{177}Hf$ in zircon as a pressure proxy: Geology, v. 51, p. 233–237, https://doi.org/10.1130/G50659.1

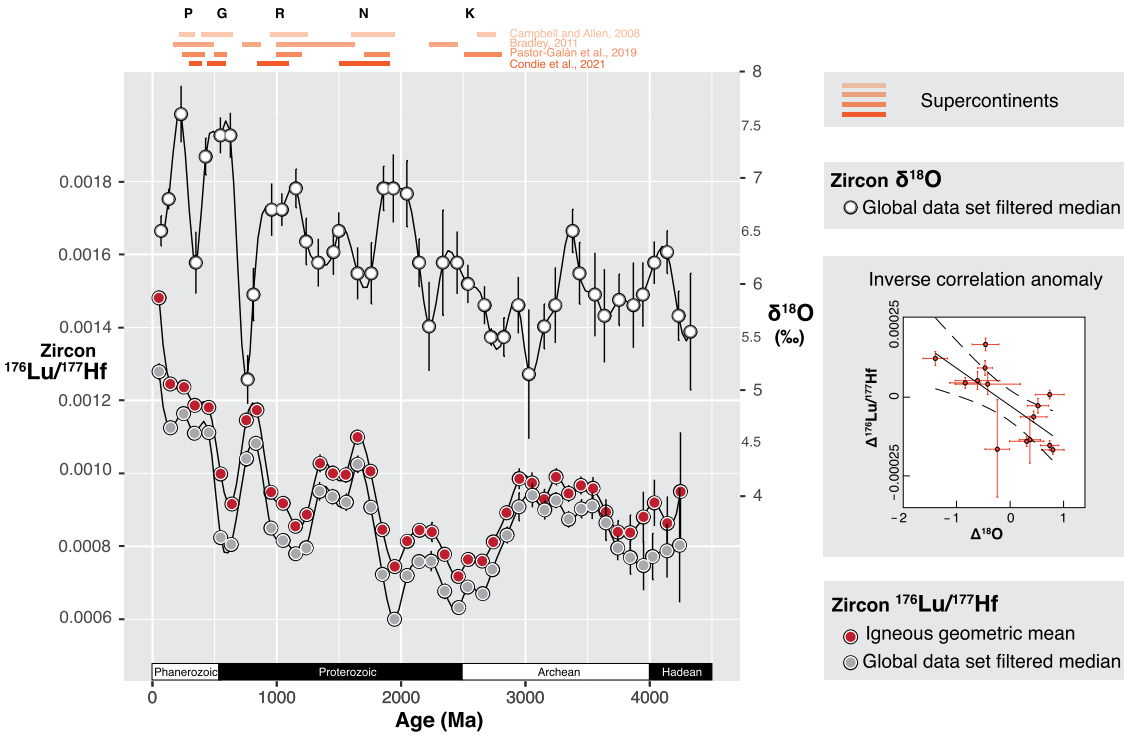

Figure 1. Secular variations of $^{176}Lu/^{177}Hf$ and $\delta^{18}O$ isotopes in zircons. Each data point represents filtered 0.1 b.y. bins in a worldwide data set ($^{176}Lu/^{177}Hf$: $n = 124,476$; $\delta^{18}O$: $n = 6294$). Error bars are 2 standard errors of values within each bin. Orange bars represent inferred periods of supercontinent amalgamation (P—Pangea, G—Gondwana, R—Rodinia, N—Nuna, K—Kenor). Inset shows statistical inverse relationship between $^{176}Lu/^{177}Hf$ and $\delta^{18}O$.

inventory in the crust may be influential factors. Zircon crystallization increases $^{176}Lu/^{177}Hf$ in the coexisting melts, and more fractionated magmas tend to have higher $^{176}Lu/^{177}Hf$ values. Thus, the $^{176}Lu/^{177}Hf$ of magmas and their zircons may be influenced by greater depths/pressures of crystallization in orogenic zones, and by the degree of fractionation as magmas ascend within the crust (Fig. 2A).

$^{176}Lu/^{177}Hf$ AND CRYSTALLIZATION DEPTH OF ZIRCON-BEARING MAGMAS

To assess the controls on $^{176}Lu/^{177}Hf$ in zircon from igneous magmas, we compiled studies with pressure estimates of zircon-bearing igneous rocks from which zircons were measured for $^{176}Lu/^{177}Hf$ isotopes. These studies generally relied on Al-in-hornblende to determine pressures of crystallization, while other petrologic/geochemical approaches were used to define pressures of magma generation (e.g., experimental petrology, thermodynamic modeling).

Zircon saturation-crystallization may occur from depths of magma generation to depths of final emplacement (Schoene et al., 2012), depending on the composition, temperature, and alkali content of the host crystal-rich magma reservoir (Boehnke et al., 2013; Laurent et al., 2020). At present, it is not possible to directly measure pressures of crystallization in zircon, but these can be estimated by analyzing mineral phases interpreted to be cogenetic with zircon crystallization (e.g., Barnes et al., 2019). Two or more minerals from a single paragenesis can show contrasting pressures of crystallization, and the reasons are often debated (e.g., Walker et al., 2013). To overcome this issue, our data set included a range of pressures from partial melting to emplacement depth estimates to better represent the complexity of transcrustal magmatic systems (Fig. 2A; Cashman et al., 2017).

The data spanned near-surface depths to ~2.0 GPa pressures and ranged in $^{176}Lu/^{177}Hf$ from 0.0005 (ultrahigh-pressure tonalites) to >0.002 (volcanic zircons). An exponential relationship of decreasing $^{176}Lu/^{177}Hf$ with increasing pressure is described in Equation 1:

$$GPa_{(sample)} = e^{\{[^{176}Lu/^{177}Hf_{(igneous\ zircon)} - 0.000711 \pm 0.000068/0.000086]/[-0.000343 \pm 0.000025/0.000023]\}}, \quad (1)$$

where $GPa_{(sample)}$ is the pressure determined for crystallization, and $^{176}Lu/^{177}Hf_{(igneous\ zircon)}$ is the geometric mean of many determinations for a sample or group of related samples from the same geologic unit. For an individual sample, the $^{176}Lu/^{177}Hf$ ratios can vary by ±25% in cogenetic zircons, whether volcanic or plutonic. As a result, ~10 or more analyses are required to estimate the mean $^{176}Lu/^{177}Hf$ and associated pressure for a given data point (Fig. 2B). One important caveat is therefore that Equation 1 is not appropriate for single-zircon pressure determinations.

Metamorphic zircons represent a modest component in the global geologic record (e.g., ~8% estimated by Balica et al., 2020). Similar to the approach for igneous zircons, we compiled data for metamorphic zircons using their age, $^{176}Lu/^{177}Hf$, and phase equilibria–determined pressure-temperature conditions (Fig. 2B). Igneous zircons with $^{176}Lu/^{177}Hf < 0.0003$ are scarce, and a large majority of metamorphic zircons have $^{176}Lu/^{177}Hf < 0.0005$ (Fig. 2C). The overlap between igneous and metamorphic zircons is therefore small, and the $^{176}Lu/^{177}Hf$ ratio can be used for screening zircons of unknown origin when internal textures are ambiguous or unavailable (see the Supplemental Material).

CONTROLS ON $^{176}Lu/^{177}Hf$ IN IGNEOUS ZIRCONS

The main sink of Hf in igneous rocks is zircon, whereas Lu is incorporated in a number of other minerals aside from garnet (e.g., amphibole, pyroxene, apatite, titanite). Lu is less compatible in zircon than Hf, and so the $^{176}Lu/^{177}Hf$ ratio is substantially lower in zircon than in the melt from which it crystallized, approximately by a factor of 5–30 (Data Set S2). Garnet has a much greater affinity for Lu, it can be abundant in the source of magmas in the middle and deep crust, and any melt generated in equilibrium with garnet is likely to have a lower $^{176}Lu/^{177}Hf$ ratio than the residue (Taylor et al., 2016; Rubatto, 2017; Gardiner et al., 2018). Other minerals such as amphibole, pyroxene, apatite, titanite, and ilmenite can influence $^{176}Lu/^{177}Hf$ in the melt, but in the presence of zircon and/or garnet, they have a minor effect on $^{176}Lu/^{177}Hf$ in the evolving magma or in zircon (see the Supplemental Material).

The $^{176}Lu/^{177}Hf$ ratio of a melt is sensitive to the melt fraction and to the proportion of garnet in the residue (Fig. 3A). Once this melt forms and starts to ascend within the crust, zircon saturation and fractionation become the dominant controls on $^{176}Lu/^{177}Hf$ in the evolving melt (assuming the lack of igneous garnet influence on the liquidus),

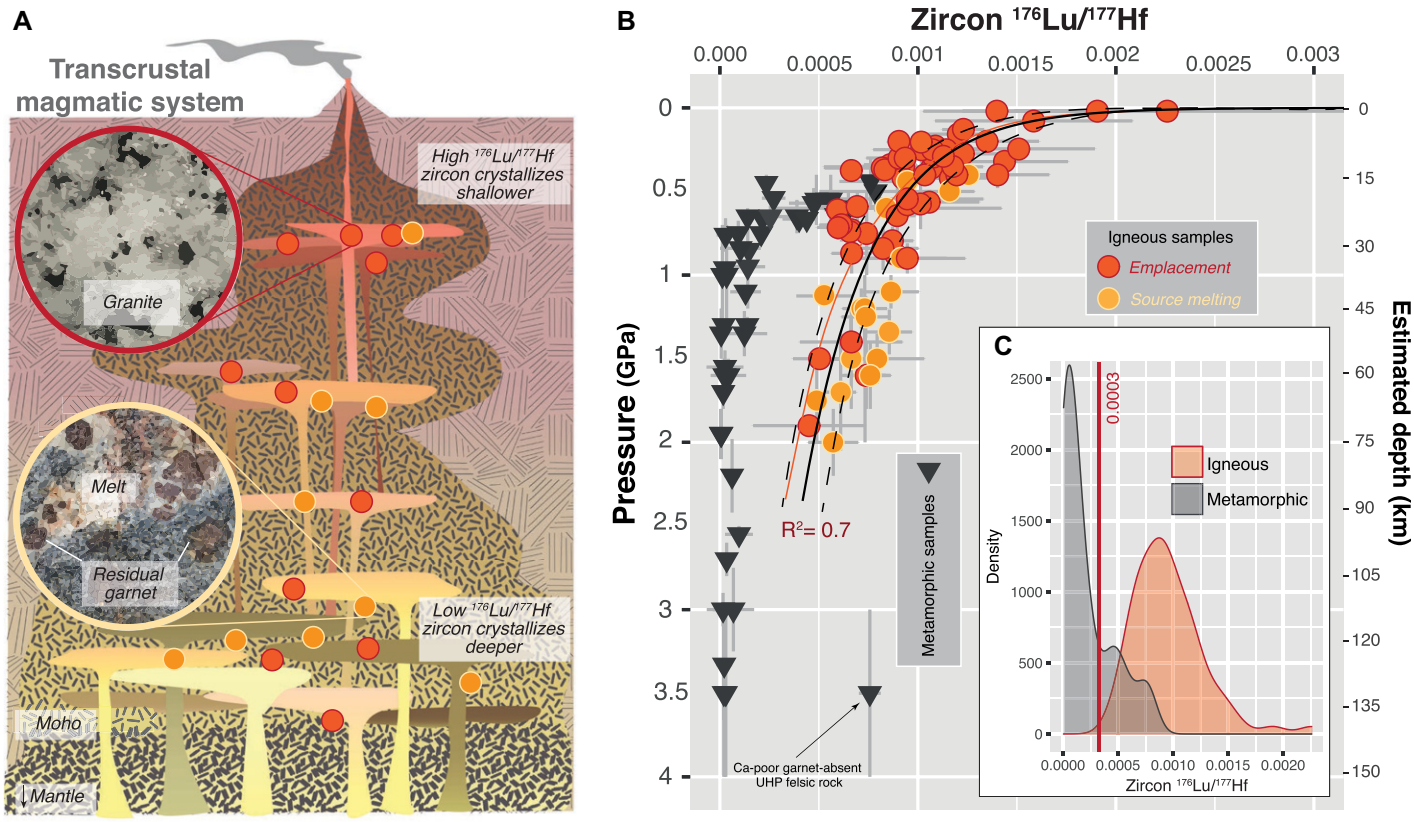

Figure 2. (A) Schematic transcrustal magmatic system (modified from Cashman et al., 2017) where melt and zircon $^{176}Lu/^{177}Hf$ compositions change with respect to garnet stability in the residue, and with magma fractionation upon ascent in the crust. (B) Compilation of Lu/Hf isotope ratios (plotted as geometric means) of 2224 zircons from igneous rocks (circles; $n = 70$), 1014 zircons from metamorphic rocks (gray triangles; $n = 44$), and estimated pressures during zircon crystallization. The best-fit curve and 95% confidence interval are shown by solid and dashed lines, respectively. The best-fit curve based on emplacement estimates only is shown by the solid red line; it makes the calculated depths shallower by a small amount that does not change our interpretations. (C) Histogram of samples used to characterize the metamorphic and igneous trends. UHP—ultrahigh-pressure.

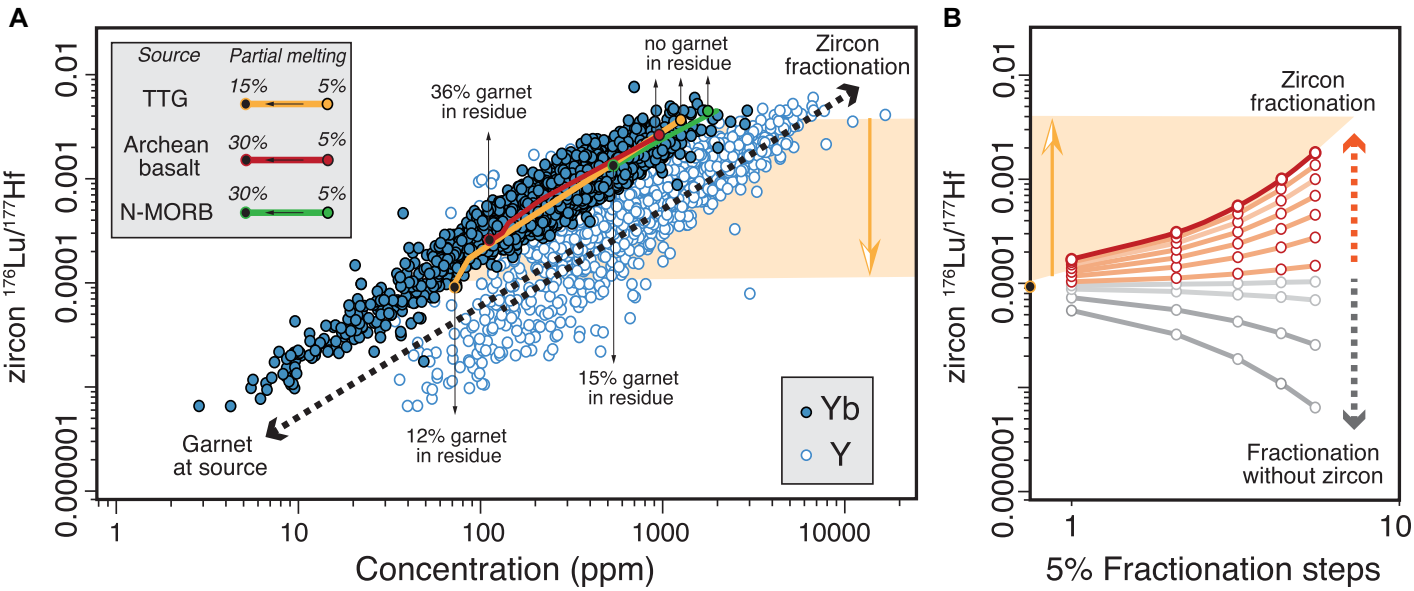

Figure 3. Geochemical controls on $^{176}Lu/^{177}Hf$ proxy. (A) Correlation between calculated zircon $^{176}Lu/^{177}Hf$ and Yb-Y concentrations for 4472 analyses. Successful partial melting models (i.e., models that overlap natural data) for three sources show coevolution of $^{176}Lu/^{177}Hf$ and Yb in zircon crystals from magmas produced with different proportions of garnet as a residual phase (Y field is shown for comparison). TTG—tonalite-trondhjemite-granodiorite; N-MORB—normal mid-ocean ridge basalt. (B) Variations in $^{176}Lu/^{177}Hf$ ratios for zircon crystallizing in melt, with two distinct trends of fractional crystallization. Gray and red paths consider subsequent 5% fractionation steps of crystallizing minerals, and red paths also account for 0.01% to 0.1% zircon fractionation. Yellow fields in both diagrams highlight similar $^{176}Lu/^{177}Hf$ variation for either process presented in A or B.

by subtracting Hf from the system (Fig. 3B). The variation of $^{176}Lu/^{177}Hf$ with pressure is therefore thought to reflect higher amounts of garnet in the source at greater depths, combined with the increase in magma fractionation with decreasing depth (Dhuime et al., 2015). Other possible factors controlling Lu/Hf variation are temperature (Claiborne et al., 2017) and potential changes in magma types through time (Laurent et al., 2014). The impact of these two factors on the $^{176}Lu/^{177}Hf$ ratio in zircon is minor (see the Supplemental Material), and we conclude that garnet as a residual phase and zircon fractionation and increasing magma fractionation with decreasing depth are the major factors that control $^{176}Lu/^{177}Hf$ variations with depth (Fig. 2). Crystallization is the dominant control on $^{176}Lu/^{177}Hf$ through most of the depth range considered (Fig. 2B), and, as such, this is the focus of the following discussion.

PLUMBING THE DEPTHS OF THE ZIRCON ARCHIVE

We applied Equation 1 to geometric means of $^{176}Lu/^{177}Hf$ from the global zircon database to calculate the apparent mean depths of crystallization of zircon-bearing igneous rocks through time (Fig. 4, red curve). The deepest mean depths of crystallization (~30–35 km) occurred at ca. 2.6 and ca. 1.9 Ga. Shallower depths (~10–15 km) are observed for the Hadean and Paleoarchean/Mesoarchean, suggesting that changes in the depths of crystallization are not simply a function of time.

Strikingly, a marked cyclicity was observed over the last 3.0 b.y., but it is absent in the earlier record (Fig. 4). The broad coincidence of troughs in the crystallization depth curve (yellow stars, associated with the lowest $^{176}Lu/^{177}Hf$ ratios) with peaks in $\delta^{18}O$ and periods of supercontinent assembly (Fig. 1) suggests a first-order link with collisional processes, such as thickening and reworking of continental crust. This pattern implies either deeper exhumation through erosional and tectonic processes associated with continental collision and thickening (Blackburn et al., 2018), more efficient entrapment of magmas at deeper levels during global compressional episodes (e.g., Loucks, 2021), or a combination of both processes. Reciprocally, the peaks in the crystallization depth curve (green stars, associated with the highest $^{176}Lu/^{177}Hf$ ratios) reflect periods of maximum shallowing during tectonic extension, as in supercontinent breakup.

An unexpected feature of Figure 4 is that both the depths of deepest crystallization (yellow stars) and the peaks of shallowest crystallization (green stars) have progressively decreased since the Neoarchean, with slopes of ~0.015 and ~0.010 km/m.y., respectively. This may be interpreted as follows: (1) The red curve is a primary signal for mean crystallization depths, with deeper magmas being more abundant during older collisional events; or (2) the progressive apparent decrease of crystallization depths is due to preferential removal of upper-crustal zircons from the global zircon archive via erosion and physical destruction. The latter hypothesis does not necessarily involve changes in the primary mean depths of crystallization.

The primary mean depth of crystallization has decreased with time since 3 Ga (Fig. 4), and this may be linked to the secular cooling of the mantle (Herzberg et al., 2010) or to changes in average crustal thickness (Tang et al., 2021), although these are complex issues to address with little consensus (e.g., Balica et al., 2020; Tamblyn et al., 2022). In contrast, cumulative erosion is known to increase with time, and in young orogens in which the upper crust remains well preserved, deeper orogenic rocks are present in smaller volumes than in older orogens (e.g., Blackburn, et al., 2018). For example, the comparison between Tibet and older orogens with more deeply eroded roots (e.g., ca. 0.6 Ga Braziliano, ca. 1.1 Ga Grenvillian, and ca. 1.9 Ga Trans-Hudson collisional orogens) revealed a much greater exposure of middle to deep crust in the older orogens (e.g., Weller et al., 2021). In addition, continental collision involves significant reworking and exhumation of deeper crustal levels that may contain ancient reworked basement and continental margin sediments. This results in a progressive removal of upper-crust zircons and exposure of the grains that crystallized at greater depths.

It is likely that the $^{176}Lu/^{177}Hf$ global zircon record has been affected by both erosion and geothermal lithospheric conditions over billions of years, and a better understanding of the observed shallowing of maximum magma crystallization depths through Earth history may involve more detailed modeling of the interaction between erosion and thermal history through the cyclical generation and destruction of supercontinents. Nonetheless, it is striking that the cycles of magma crystallization depths started in response to global supercontinent activity between 3.0 and 2.5 Ga, which may be further evidence that plate tectonics became global at that time.

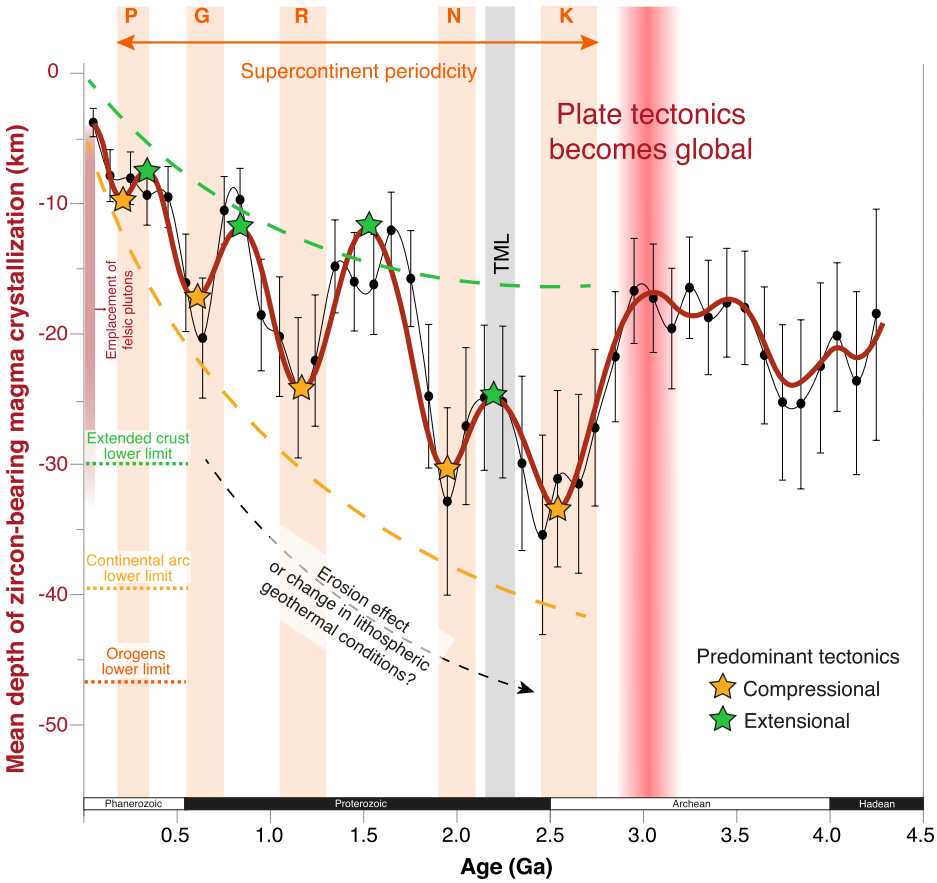

Figure 4. Secular variation in the mean depth of zircon-bearing magmas. Smoothed red curve is based on the 20th-order polynomial function of the $^{176}Lu/^{177}Hf$ geomean of 0.1 b.y. bins (black thin curve). Depths of felsic magmas in the present-day continental crust are presented for comparison (Jagoutz and Kelemen, 2015). Vertical orange bars represent the periods of supercontinents peak assembly as inferred from this study (P—Pangea, G—Gondwana, R—Rodinia, N—Nuna, K—Kenor; references are given in the Supplemental Material [see footnote 1]). Vertical gray bar represents the tectono-magmatic lull (TML) interval (Spencer et al., 2018). Lower limit of crust thickness estimates from Christensen and Mooney (1995) are plotted as horizontal dashed lines for comparison.

ACKNOWLEDGMENTS

This project was funded by the European Research Council under the European Union's Horizon 2020 research and innovation program (no. 817934). We thank the anonymous reviewers, Steven L. Goldstein, and Oscar Laurent for constructive and insightful comments that allowed us to clarify the manuscript. We also thank Urs Schaltegger for very helpful editorial guidance.

REFERENCES CITED

Annen, C., Blundy, J.D., and Sparks, R.S.J., 2006, The genesis of intermediate and silicic magmas in deep crustal hot zones: Journal of Petrology, v. 47, p. 505–539, https://doi.org/10.1093/petrology/egi084.

Balica, C., Ducea, M.N., Gehrels, G.E., Kirk, J., Roban, R.D., Luffi, P., Chapman, J.B., Triantafyllou, A., Guo, J., Stoica, A.M., and Ruiz, J., 2020, A zircon petrochronologic view on granitoids and continental evolution: Earth and Planetary Science Letters, v. 531, https://doi.org/10.1016/j.epsl.2019.116005.

Barnes, C.G., Werts, K., Memeti, V., and Ardill, K., 2019, Most granitoid rocks are cumulates: Deductions from hornblende compositions and zircon saturation: Journal of Petrology, v. 60, p. 2227–2240, https://doi.org/10.1093/petrology/egaa008.

Belousova, E.A., Kostitsyn, Y.A., Griffin, W.L., Begg, G.C., O'Reilly, S.Y., and Pearson, N.J., 2010, The growth of the continental crust: Constraints from zircon Hf-isotope data: Lithos, v. 119, p. 457–466, https://doi.org/10.1016/j.lithos.2010.07.024.

Blackburn, T., Ferrier, K.L., and Perron, J.T., 2018, Coupled feedbacks between mountain erosion rate, elevation, crustal temperature, and density: Earth and Planetary Science Letters, v. 498, p. 377–386, https://doi.org/10.1016/j.epsl.2018.07.003.

Boehnke, P., Watson, E.B., Trail, D., Harrison, T.M., and Schmitt, A.K., 2013, Zircon saturation re-revisited: Chemical Geology, v. 351, p. 324–334, https://doi.org/10.1016/j.chemgeo.2013.05.028.

Bradley, D.C., 2011, Secular trends in the geologic record and the supercontinent cycle: Earth-Science Reviews, v. 108, p.16–33, https://doi.org/10.1016/j.earscirev.2011.05.003.

Brown, M., 1994, The generation, segregation, ascent and emplacement of granite magma: The migmatite-to-crustally-derived-granite connection in thickened orogens: Earth-Science Reviews, v. 36, p. 83–130, https://doi.org/10.1016/0012-8252(94)90009-4.

Campbell, I.H., and Allen, C.M., 2008, Formation of supercontinents linked to increases in atmospheric oxygen: Nature Geoscience, v. 1, p.554–558, https://doi.org/10.1038/ngeo259.

Cashman, K.V., Sparks, R.S.J., and Blundy, J.D., 2017, Vertically extensive and unstable magmatic systems: A unified view of igneous processes: Science, v. 355, https://doi.org/10.1126/science.aag3055.

Christensen, N.I., and Mooney, W.D., 1995, Seismic velocity structure and composition of the continental crust: A global view: Journal of Geophysical Research: Solid Earth, v. 100, p. 9761–9788, https://doi.org/10.1029/95JB00259.

Claiborne, L.L., Miller, C.F., Gualda, G.A., Carley, T.L., Covey, A.K., Wooden, J.L., and Fleming, M.A., 2017, Zircon as magma monitor: Robust, temperature-dependent partition coefficients from glass and zircon surface and rim measurements from natural systems, *in* Moser, D.E., et al., eds., Microstructural Geochronology: Planetary Records Down to Atom Scale: American Geophysical Union Geophysical Monograph 232, p. 1–33, https://doi.org/10.1002/9781119227250.ch1.

Condie, K.C., Pisarevsky, S.A., and Puetz, S.J., 2021, LIPs, orogens and supercontinents: The ongoing saga: Gondwana Research, v. 96, p.105–121, https://doi.org/10.1016/j.gr.2021.05.002.

Dhuime, B., Hawkesworth, C.J., Cawood, P.A., and Storey, C.D.A., 2012, Change in the geodynamics of continental growth 3 billion years ago: Science, v. 335, p. 1334–1336, https://doi.org/10.1126/science.1216066.

Dhuime, B., Wuestefeld, A., and Hawkesworth, C.J., 2015, Emergence of modern continental crust about 3 billion years ago: Nature Geoscience, v. 8, p. 552–555, https://doi.org/10.1038/ngeo2466.

Gardiner, N.J., Kirkland, C.L., and Van Kranendonk, M.J., 2016, The juvenile hafnium isotope signal as a record of supercontinent cycles: Scientific Reports, v. 6, https://doi.org/10.1038/srep38503.

Gardiner, N.J., Johnson, T.E., Kirkland, C.L., and Smithies, R.H., 2018, Melting controls on the lutetium-hafnium evolution of Archaean crust: Precambrian Research, v. 305, p. 479–488, https://doi.org/10.1016/j.precamres.2017.12.026.

Herzberg, C., Condie, K., and Korenaga, J., 2010, Thermal history of the Earth and its petrological expression: Earth and Planetary Science Letters, v. 292, p. 79–88, https://doi.org/10.1016/j.epsl.2010.01.022.

Hogan, J.P., and Gilbert, M.C., 1995, The A-type Mount Scott granite sheet: Importance of crustal magma traps: Journal of Geophysical Research: Solid Earth, v. 100, p. 15,779–15,792, https://doi.org/10.1029/94JB03258.

Jagoutz, O., and Kelemen, P.B., 2015, Role of arc processes in the formation of continental crust: Annual Review of Earth and Planetary Sciences, v. 43, p. 363–404, https://doi.org/10.1146/annurev-earth-040809-152345.

Laurent, O., Martin, H., Moyen, J.F., and Doucelance, R., 2014, The diversity and evolution of late-Archean granitoids: Evidence for the onset of "modern-style" plate tectonics between 3.0 and 2.5 Ga: Lithos, v. 205, p. 208–235, https://doi.org/10.1016/j.lithos.2014.06.012.

Laurent, O., Björnsen, J., Wotzlaw, J.F., Bretscher, S., Pimenta Silva, M., Moyen, J.F., Ulmer, P., and Bachmann, O., 2020, Earth's earliest granitoids are crystal-rich magma reservoirs tapped by silicic eruptions: Nature Geoscience, v. 13, p. 163–169, https://doi.org/10.1038/s41561-019-0520-6.

Loucks, R.R., 2021, Deep entrapment of buoyant magmas by orogenic tectonic stress: Its role in producing continental crust, adakites, and porphyry copper deposits: Earth-Science Reviews, v. 220, https://doi.org/10.1016/j.earscirev.2021.103744, corrigendum available at https://doi.org/10.1016/j.earscirev.2021.103821.

McKenzie, N.R., Smye, A.J., Hegde, V.S., and Stockli, D.F., 2018, Continental growth histories revealed by detrital zircon trace elements: A case study from India: Geology, v. 46, p. 275–278, https://doi.org/10.1130/G39973.1.

O'Brien, T.M., and Miller, E.L., 2014, Continuous zircon growth during long-lived granulite facies metamorphism: A microtextural, U-Pb, Lu-Hf and trace element study of Caledonian rocks from the Arctic: Contributions to Mineralogy and Petrology, v. 168, https://doi.org/10.1007/s00410-014-1071-x.

Pastor-Galán, D., Nance, R.D., Murphy, J.B., and Spencer, C.J., 2019, Supercontinents: myths, mysteries, and milestones, *in* Wilson, R.W., eds., Fifty Years of the Wilson Cycle Concept in Plate Tectonics: Geological Society, London, Special Publication 470, p. 39–64, https://doi.org/10.1144/SP470.16.

Petford, N., Cruden, A.R., McCaffrey, K.J.W., and Vigneresse, J.L., 2000, Granite magma formation, transport and emplacement in the Earth's crust: Nature, v. 408, p. 669–673, https://doi.org/10.1038/35047000.

Rubatto, D., 2017, Zircon: The metamorphic mineral, *in* Kohn, M.J., et al., eds., Petrochronology: Methods and Applications: Reviews in Mineralogy & Geochemistry, v. 83, p. 261–296, https://doi.org/10.1515/9783110561890-010.

Schoene, B., Schaltegger, U., Brack, P., Latkoczy, C., Stracke, A., and Günther, D., 2012, Rates of magma differentiation and emplacement in a ballooning pluton recorded by U-Pb TIMS-TEA, Adamello batholith, Italy: Earth and Planetary Science Letters, v. 355–356, p. 162–173, https://doi.org/10.1016/j.epsl.2012.08.019.

Spencer, C.J., Cawood, P.A., Hawkesworth, C.J., Raub, T.D., Prave, A.R., and Roberts, N.M., 2014, Proterozoic onset of crustal reworking and collisional tectonics: Reappraisal of the zircon oxygen isotope record: Geology, v. 42, p. 451–454, https://doi.org/10.1130/G35363.1.

Spencer, C.J., Murphy, J.B., Kirkland, C.L., Liu, Y.B., and Mitchell, R.N., 2018, A Palaeoproterozoic tectono-magmatic lull as a potential trigger for the supercontinent cycle: Nature Geoscience, v. 11, p. 97–101, https://doi.org/10.1038/s41561-017-0051-y.

Tamblyn, R., Hasterok, D., Hand, M., and Gard, M., 2022, Mantle heating at ca. 2 Ga by continental insulation: Evidence from granites and eclogites: Geology, v. 50, p. 91–95, https://doi.org/10.1130/G49288.1.

Tang, M., Ji, W.Q., Chu, X., Wu, A.B., and Chen, C., 2021, Reconstructing crustal thickness evolution from europium anomalies in detrital zircons: Geology, v. 49, p. 76–80, https://doi.org/10.1130/G47745.1.

Taylor, R.J.M., Kirkland, C.L., and Clark, C., 2016, Accessories after the facts: Constraining the timing, duration and conditions of high-temperature metamorphic processes: Lithos, v. 264, p. 239–257, https://doi.org/10.1016/j.lithos.2016.09.004.

Thybo, H., and Nielsen, C.A., 2009, Magma-compensated crustal thinning in continental rift zones: Nature, v. 457, p. 873–876, https://doi.org/10.1038/nature07688.

Vigneresse, J.L., Tikoff, B., and Ameglio, L., 1999, Modification of the regional stress field by magma intrusion and formation of tabular granitic plutons: Tectonophysics, v. 302, p. 203–224, https://doi.org/10.1016/S0040-1951(98)00285-6.

Voice, P.J., Kowalewski, M., and Eriksson, K.A., 2011, Quantifying the timing and rate of crustal evolution: Global compilation of radiometrically dated detrital zircon grains: The Journal of Geology, v. 119, p. 109–126, https://doi.org/10.1086/658295.

Walker, B.A., Klemetti, E.W., Grunder, A.L., Dilles, J.H., Tepley, F.J., and Giles, D., 2013, Crystal reaming during the assembly, maturation, and waning of an eleven-million-year crustal magma cycle: Thermobarometry of the Aucanquilcha volcanic cluster: Contributions to Mineralogy and Petrology, v. 165, p. 663–682, https://doi.org/10.1007/s00410-012-0829-2.

Weller, O.M., Mottram, C.M., St-Onge, M.R., Möller, C., Strachan, R., Rivers, T., and Copley, A., 2021, The metamorphic and magmatic record of collisional orogens: Nature Reviews: Earth & Environment, v. 2, p. 781–799, https://doi.org/10.1038/s43017-021-00218-z.

Printed in USA